Hybrid Titanium Catalyst Supported on Core-Shell Silica/Poly(styrene-*co*-acrylic acid) Carrier

Lijun Du, Wei Li, Lina Fan, Binbo Jiang, Jingdai Wang, Yongrong Yang, Zuwei Liao

State Key Laboratory of Chemical Engineering, Department of Chemical and Biochemical Engineering, Zhejiang University, Hangzhou 310027, People's Republic of China

Received 23 October 2009; accepted 1 March 2010
DOI 10.1002/app.32374
Published online 7 June 2010 in Wiley InterScience (www.interscience.wiley.com).

ABSTRACT: Hybrid titanium catalysts supported on silica/poly(styrene-*co*-acrylic acid) (SiO_2/PSA) core-shell carrier were prepared and studied. The resulting catalysts were characterized by Fourier transform infrared (FTIR) spectroscopy, laser scattering particle analyzer and scanning electronic microscope (SEM). The hybrid catalyst ($TiCl_3/MgCl_2/THF/SiO_2{\cdot}TiCl_4/MgCl_2$/PSA) showed core-shell structure and the thickness of the PSA layer in the two different hybrid catalysts was 2.0 μm and 5.0 μm, respectively. The activities of the hybrid catalysts were comparable to the conventional titanium-based Ziegler-Natta catalyst ($TiCl_3/MgCl_2/THF/SiO_2$). The hybrid catalysts showed lower initial polymerization rate and longer polymerization life time compared with $TiCl_3/MgCl_2/THF/SiO_2$. The activities of the hybrid catalysts were enhanced firstly and then decreased with increasing $P_{H_2}/P_{C_2H_4}$. Higher molecular weight and broader molecular weight distribution (MWD) of polyethylene produced by the core-shell hybrid catalysts were obtained. Particularly, the hybrid catalyst with a PSA layer of 5.0 μm obtained the longest polymerization life time with the highest activity (2071 kg PE mol^{-1} Ti h^{-1}) and the resulting polyethylene had the broadest MWD (polydispersity index = 11.5) under our experimental conditions. The morphology of the polyethylene particles produced by the hybrid catalysts was spherical, but with irregular subparticles due to the influence of PSA layer. © 2010 Wiley Periodicals, Inc. J Appl Polym Sci 118: 1743–1751, 2010

Key words: hybrid titanium catalyst; core-shell structure; ethylene polymerization; kinetic curve; broad molecular weight distribution

INTRODUCTION

Various methods have been proposed to design special catalysts to obtain tailor-made polymers with improved properties and easier processability, such as broad and bimodal molecular weight distribution (MWD) polyethylene.[1–4] Currently, combining multicomponent catalysts on one support to produce polyethylene with different molecular weight (MW) ranges has received considerable attention by researchers.[5–11] Soares and coworkers[5] combined different types of metallocene catalysts, such as $Et[Ind]_2ZrCl_2$ and Cp_2HfCl_2, onto a single MAO pretreated silica support to produce polyethylene. Although the resulting polyethylene could obtain broader or bimodal MWD, the polydispersity index (PDI) was still less than 7. Santos and coworkers tried to immobilize metallocene catalyst $CpTiCl_3$ on $MgCl_2$ supported Ziegler-Natta catalyst[7] and evaluated the Ziegler-Natta/Metallocene hybrid catalyst behavior in an ethylene-1-butene copolymerization slurry process.[8] They concentrated on the characterization of the catalyst and didn't provide MW or MWD of the obtained polyethylene. Lee and coworkers[9–11] also obtained hybrid catalysts by combining Ziegler-Natta and metallocene catalysts on $SiO_2/MgCl_2$ bisupport and the resulting polyethylene showed two melting temperatures and a bimodal MWD.

Obviously, the cost-effective hybrid catalyst systems provide high potential to produce polyethylene with broad MWD or bimodal MWD. However, the optimum hybrid catalyst technique is hard to achieve due to some rigorous requirements: balanced activity in polymerization conditions; long and stable polymerization life time; difference in MW of polymers from each active species; good and balanced hydrogen, alkyl art, and comonomer response; and good polymer morphology.[12] They should also be kinetically and chemically compatible.[12] Breakthroughs in catalyst support material may be able to achieve the requirements.

Core-shell particles, containing inorganic particles as core and organic materials as shell, are attracting

Correspondence to: Z. Liao (liaozw@zju.edu.cn).

Contract grant sponsor: The Project of National Natural Science Foundation of China; contract grant numbers: 20776124, 20736011.

Contract grant sponsor: National High Technology Research and Development Program of China; contract grant number: 2007AA030208.

a great deal of interest in material science field[13–18] and have been used as the support of heterogeneous catalysts.[19–23] The core-shell hybrid supports often exhibit improved properties over their single-component counterparts. Liu et al.[21] immobilized Cp_2ZrCl_2 on the core-shell support which was directly prepared by combining poly(styrene-*co*-4-vinylpyridine) on the surface of silica in the presence of (3-Aminnopropyl)triethoxysilane. The catalysts maintained good activity and offered polyethylene particles with the required morphology and higher bulk density than the polyethylene obtained from Cp_2ZrCl_2 supported on polymer. Guo et al.[22] synthesized a kind of core-shell support by copolymerizing 3-(trimethoxysilyl)propyl methacrylate and 4-vinypridine on the surface of silica. Cp_2ZrCl_2 was then anchored on the core-shell support and ethylene polymerization was conducted. They found that the catalyst supported on core-shell particles showed higher activity than that on silica. Zhang and Jin[23] prepared SiO_2-supported polystyrene-incorporated nickel^{II} α-diimine catalysts for ethylene polymerization. They concluded that the catalysts exhibited high activity and the resulting polyethylene showed improved particle morphology. However, the core-shell particles were only used to support single catalyst in these articles. As far as we know, using core-shell particles to support hybrid catalysts were not published.

Our approach involves the formation of the polymer-coated carrier following the phase inversion principles.[16] Furthermore, two individual catalysts are supported on the polymer-coated carrier to produce polyethylene with broad MWD through a normal polymerization. The polymer shell not only serves as the support to anchor one catalyst but also separates the hybrid catalyst into two independent regions. As a result, it is feasible to supply the suitable reaction conditions for the two individual catalysts respectively. In this article silica/poly(styrene-*co*-acrylic acid) (SiO_2/PSA) inorganic/organic core-shell carriers were prepared to support two different Ziegler-Natta catalysts. Hybrid catalysts ($TiCl_3$/$MgCl_2$/THF/SiO_2·$TiCl_4$/$MgCl_2$/PSA) were obtained to allow normal gas-phase ethylene polymerization. The conventional titanium-based Ziegler-Natta catalyst ($TiCl_3$/$MgCl_2$/THF) supported on silica was also prepared for comparison. The influences of the PSA layer in hybrid catalysts on ethylene polymerization behavior and the properties of produced polyethylene were investigated.

EXPERIMENTAL

Materials

All experimental operations involving air- or moisture-sensitive compounds were carried out under a nitrogen atmosphere using a standard Schlenk technique. High-purity nitrogen, polymerization-grade ethylene and hydrogen were obtained from SINOPEC Shanghai Corporation (Shanghai, China) and purified by sequentially passing them through copper catalyst column and alumina column. Solvents (isopentane, *n*-hexane, and tetrahydrofuran) were dried over 4 Å molecular sieves for at least 10 days and then purified by solvent purification system of Innovative Technology. Silica 2485 from W. R. Grace & Co., was activated at 600°C for 4 h with nitrogen flow. Magnesium chloride ($MgCl_2$, 97.5% wt, H_2O—2% max), aluminum chloride -titanium trichloride complex ($AlCl_3$·$3TiCl_3$, 98% wt) and titanium (IV) chloride ($TiCl_4$, ≥98.0% wt) were purchased from J&K Company and used without further treatment. Triethylaluminium (TEA) was purchased from Aldrich. Poly(styrene-*co*-acrylic acid) (PSA) provided by Changchun Institute of Applied Chemistry , Chinese Academy of Science, was dried at 70°C under nitrogen flow for 24 h before use.

Preparation of catalysts

In a typical catalyst preparation, the catalyst was prepared in a three-step process:

Step 1: Under a dry nitrogen atmosphere, silica (6.0 g) and hexane (40 mL) were stirred in a 200 mL Schlenk flask. The flask was placed in an oil bath (55°C). TEA (2.8 mmol) was added to the stirred silica slurry at 55°C and the reaction continued for about 2 h. The solvent was removed by evaporation under nitrogen flow to obtain a free-flowing powder. $MgCl_2$ (0.6 g) and $AlCl_3$·$3TiCl_3$ (0.5 g) were placed in another 200 mL Schlenk flask equipped with magnetic stirrer and refluxed in tetrahydrofuran (THF) until dissolution was completed. The solution was then cooled to room temperature. The above treated silica was added to this solution. The mixture was agitated for 2 h and excess THF was distilled. The residual solid was dried for 3 h at 65°C under a nitrogen flow and finally pink free-flowing powders were obtained. This was a kind of conventional heterogeneous Ziegler-Natta catalyst ($TiCl_3$/$MgCl_2$/THF/SiO_2).

Step 2: Under a dry nitrogen atmosphere, PSA (2.5 g) and $MgCl_2$ (0.3 g) were dissolved in THF solution (100 mL) and stirred for 6 h at 60°C, to prepare the PSA/$MgCl_2$/THF solution. The mixture of the catalyst obtained in step 1 (4.0 g) and the PSA/$MgCl_2$/THF solution (32 mL) were stirred in a 250 mL Schlenk flask at 150 rpm at 0°C. Isopentane (160 mL) was heated to 35°C in another flask and then isopentane vapor slowly diffused into the mixture. The phase inversion process involved a phase separation of the polymer solution.[24,25] Then the precipitation of PSA/$MgCl_2$ on $TiCl_3$/$MgCl_2$/THF/SiO_2 took place.

After all the isopentane diffused into the mixture (160 min), the residual solids were separated, washed three times with 120 mL hexane at room temperature and then dried at 50°C under nitrogen flow for 2 h. White free-flowing PSA-coated catalyst was then obtained.

Step 3: Under an inert atmosphere of dry nitrogen, 2.0 g of PSA-coated catalyst and hexane (40 mL) were added to a 200 mL Schlenk flask containing a magnetic stirring bar. $TiCl_4$ (0.26 g) was added via syringe to the stirred mixture. After 30 min, the liquid phase was removed by evaporation under nitrogen flow at 55°C, to obtain pale yellow free-flowing hybrid catalyst ($TiCl_3/MgCl_2/THF/SiO_2{\cdot}TiCl_4/MgCl_2/PSA$).

These catalysts prepared by the method described above were respectively denoted as HC-0 (the catalyst without PSA, $PSA/SiO_2 = 0\%$ wt), HC-5 (one hybrid catalyst, $PSA/SiO_2 = 5\%$ wt), and HC-20 (the other hybrid catalyst, $PSA/SiO_2 = 20\%$ wt).

Ethylene homopolymerization

Ethylene homopolymerization in gas phase was carried out in a stirred 1 L Büchi stainless steel autoclave reactor, equipped with mechanical stirrer, a mass flow meter and a temperature control unit comprising cooling water and an electric heater. The reactor was heated above 90°C for more than 4 h and repeatedly pressurized with nitrogen, purged and evacuated (<10 mbar) before polymerization. The polymerization temperature was 88°C. The catalyst was introduced into the reactor under nitrogen purging after the injection of appropriate TEA as cocatalyst. Hydrogen was allowed to be measured and added by following the pressure increase in the reactor to the prescribed content. The polymerization then occurred by loading the reactor with ethylene. The flow rate of ethylene was continuously monitored with a mass flow meter when the pressure in the reactor was closed to 9.0 bar. During polymerization, the impeller stirrer was used at 1600 rpm. The polymerizations were terminated after 4 h by venting the gaseous monomer.

Characterization

Fourier transform infrared (FTIR) spectrometry measurements were carried out on a Nicolet 5700 spectrometer. Dry samples were completely mixed with analytical grade KBr and then pressed into a form of tablet. The particle size distribution of different catalysts was determined by a laser scattering particle analyzer (Mastersizer 2000). The morphology of the catalysts was observed using a field emission scan electron microscope (SEM) (Hitachi S-4700) and the morphology of polyethylene was observed by another type of SEM (Hitachi TM-1000). The content of titanium in the catalysts was determined by ultraviolet spectroscopy (UV). UV measurements were carried out in 10-mm quartz glass cells on Unico UV-2102PC spectrophotometer. The intensity of a peak at 410 nm was used to quantify the titanium content. MW and MWD of the resulting polyethylene were measured by gel permeation chromatography (GPC) in a PL-220 instrument with 1,2, 4-trichlorobenzene as the solvent at 150°C. The universal calibration curve, obtained from narrow MWD polystyrene standards, was used to quantify the results. Melt flow indexes (MFI) were determined in a fusion index instrument (CEAST, Italy) at 190°C, using a 21.6 kg charge. Differential scanning calorimetry (DSC) measurement was performed on a Perkin–Elmer 7 series thermal analyzer with indium as the calibration standard. The nascent powder of the polyethylene was heated to 160°C (10°C/min), held at 160°C for 1 min, cooled to 50°C (10°C/min) and held at 50°C for 1 min. Finally, the polyethylene was heated to 160°C (10°C/min) again. The reported DSC curves were from the second heat cycle and the melting point was represented by the peak value.

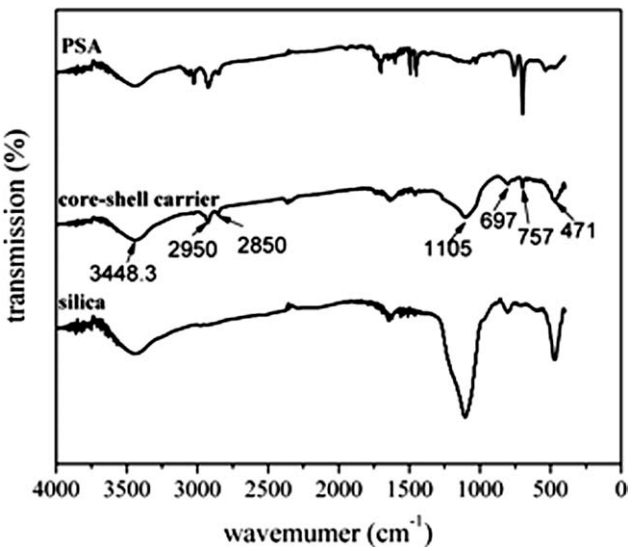

Figure 1 FTIR spectra of the carrier particles.

RESULTS AND DISCUSSION

Catalyst characterization results

Proof of the composite nature of the core-shell carrier is provided by FTIR spectra, as shown in Figure 1. Catalysts were not supported on the silica and core-shell particles for simplifying and clearly discriminating the spectra. The typical PSA absorption-bands at 757 and 697 cm^{-1}, which correspond to the phenyl C—H out-of-plane bending and benzene out-of-plane ring bending respectively [Fig. 1(a)], are

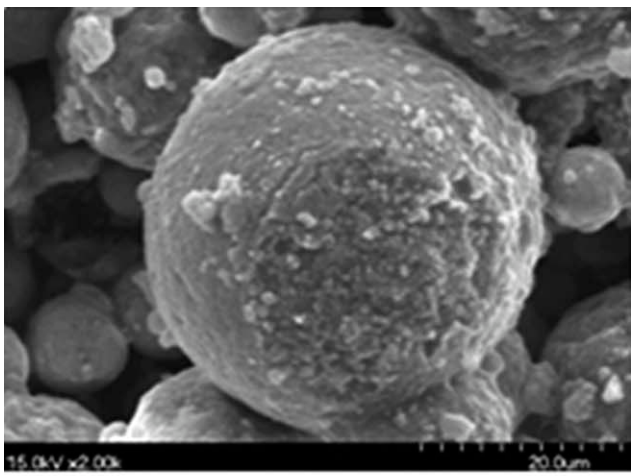

(a)

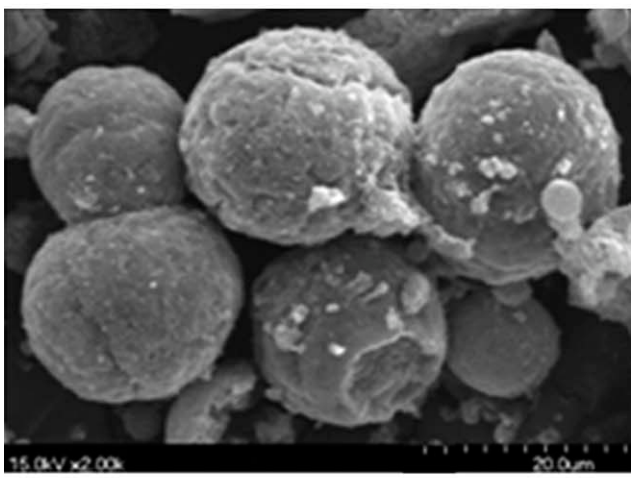

(b)

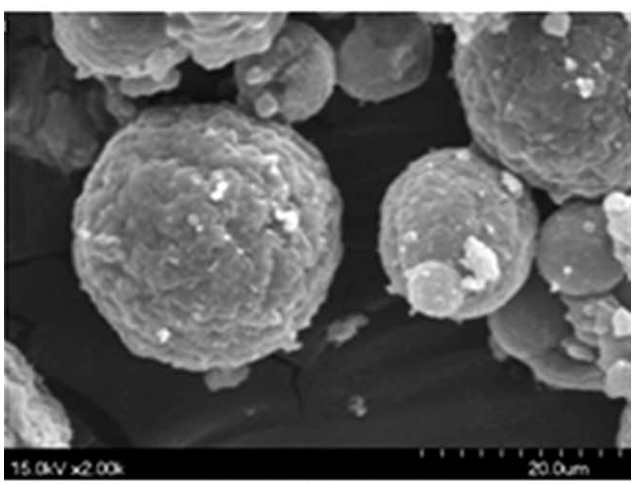

(c)

Figure 2 The SEM photographs of different catalysts (a) HC-0, (b) HC-5, and (c) HC-20.

clearly observed in the spectrum of the core-shell carrier [Fig. 1(b)]. Aliphatic C—H stretching resonances of PSA (2850–2950 cm^{-1}) can also be seen in the core-shell carrier spectrum. The typical silica absorption peaks at 1105 cm^{-1} (the asymmetrical stretching of Si—O—Si bond) and at 471 cm^{-1} (the bending vibration of Si—O bond) [Fig. 1(c)] are much weaker in core-shell particles than in silica, which confirms that these silica particles are located mainly in the interior part.

Figure 2 is the SEM photographs of different catalysts. The surface morphologies of the hybrid catalysts particles are obviously different from the catalyst without PSA layer. The particles of HC-0 are spherical in shape and smooth on the surface, but a layer of irregular and rough material covers on HC-0 after being subjected to the PSA layer formation process. Furthermore, the sponge-like wrapping layer of HC-20 is rougher and more irregular than HC-5, which suggests more PSA exist in HC-20.

The particle size distribution results in Figure 3 clearly show that the catalysts exhibit varying diameters depending on the content of PSA, which agrees well with others' investigation on core-shell spheres.[18] The average diameter of the particles increases with the content of PSA in the catalyst, which is 23.2, 27.2, and 33.3 μm corresponding to HC-0 (PSA/SiO_2 = 0% wt), HC-5 (PSA/SiO_2 = 5% wt), and HC-20 (PSA/SiO_2 = 20% wt). Therefore, the PSA layer thickness of HC-5 and HC-20 are 2.0 μm and 5.0 μm, respectively. The increase of the diameter (i.e., the thickness of PSA layer) with the content of PSA is simply due to the fact that more PSA is precipitated on the catalyst. The particle size distribution of core-shell particles becomes narrow as the content of PSA increases, indicating that most PSA are coating on the silica, not forming small pure PSA particles.

The results of FTIR, SEM photos and particle size distribution indicate that it is feasible to obtain polymer-coated particles based on phase inversion principles. Moreover, the thickness of the PSA layer can

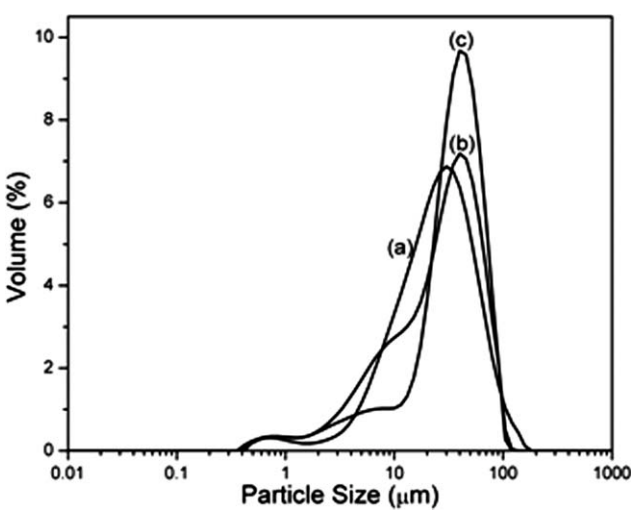

Figure 3 Particle size distribution of different catalysts (a) HC-0, (b) HC-5, and (c) HC-20.

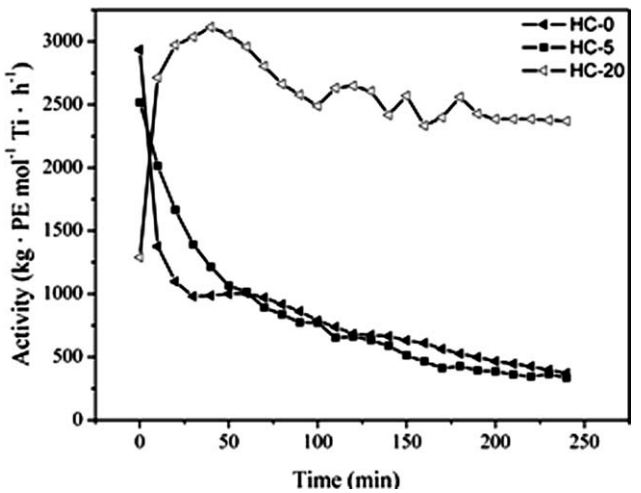

Figure 4 Ethylene homopolymerization kinetics of different catalysts.

be regulated by its content in hybrid catalysts. According to the aforementioned results, the mechanism of the formation of core-shell particles is given as follows. As the phase inversion process involves polymer transformation from a liquid to a solid state, the solidification is initiated by the transition from one liquid state into two liquids (liquid–liquid demixing).[24] In this work, isopentane vapor was slowly introduced into the mixture of the core particles and PSA/THF solution, dispersing homogeneously in the mixture. THF could be extracted into isopentane little by little. The phase inversion of the polymer solution slowly proceeds. The high polymer concentration liquid would adhere to the core material and then PSA would solidify on the surface of the core particles at a certain stage during demixing,[24,25] forming the core-shell particles. Due to the PSA layer, the polymer-coated catalysts show increasing diameter and sponge-like surface morphology.

The kinetic curve of ethylene polymerization

Ethylene homopolymerization in gas phase was carried out to investigate the influences from the PSA layer on polymerization behavior of the hybrid catalysts and the properties of the resulting polymer. Figure 4 provides the kinetic profiles of ethylene homopolymerization, indicating that the thickness of the PSA layer strongly affects the trend of the kinetic curves. HC-0 and HC-5 show a similar kinetic profile, characterized by an initial peak followed by a fast decay and then by a relatively long pseudostationary period. However, HC-20 with the PSA layer of 5.0 μm obtains kinetic curve with steadier and longer polymerization life time than the other two catalysts. The instantaneous activity of HC-20 achieves the maximum when the polymerization time is 40 min, and then decreases gradually, following almost constant from 80 min to the end of the polymerization. Hydrogen, ethylene and TEA are able to directly contact the active centers of HC-0 and HC-5 with thin PSA layer, leading to relatively high activity in the initiation stage of polymerization. The activity then decays dramatically because a large amount of polyethylene is produced on the surface of the catalysts and blocks the diffusion of reactants. Przybyla et al.[26] also found that the ethylene/1-hexene copolymer exhibited a barrier effect on the diffusion of reactants when they investigated the copolymerization of silica-supported metallocene catalysts. However, reactants (especially TEA) slowly diffuse through the PSA layer to contact the interior active sites of HC-20 because the PSA layer is thicker and serves as an effective diffusion barrier layer for the reactants. So the polymerization enters a diffusion-controlled inductive period initially. As polymerization proceeds, more reactants contact the interior sites and the activity increases slowly until the maximum is reached after about 40 min. The gradual reduction in activity for the rest time of polymerization may be attributed to several causes, including slow consumption of active sites and less reactants diffusing into interior sites because of reduced permeability of the producing polyethylene. The activity oscillates significantly in the second half stage of the polymerization, owing to the unstable diffusion behavior of the reactants through the PSA layer.

Catalytic activities

Table I lists the activities of different catalysts and the physical properties of the produced polyethylene. The titanium contents in the hybrid catalysts are a little higher than the catalyst without PSA because the functional group (—COOH) on PSA could coordinate with $TiCl_4$.[27] The activity, expressed in terms of kg polyethylene per mol of Ti per hour, is calculated based on a 4-h polymerization. The activity of HC-20 is superior to that of HC-5 and HC-0 under the same polymerization condition. The thickness of the PSA layer in each catalyst is mainly responsible for the different activities. As the thicker PSA layer in HC-20 slowed down the diffusion of the reactants, less polyethylene is produced to block the diffusion of reactants in the beginning of polymerization. The active centers of HC-20 would gradually expose to the reactants and could serve for the reaction until the end of the polymerization process, leading to the higher activity of HC-20. However, most active centers of HC-0 and HC-5 with thin PSA layer expose to the reactants at the initial stage of polymerization. The primary activities of HC-0 and HC-5 could be high enough to produce polyethylene coating on the surface of catalysts, which block the pore of the catalysts. Then the reactants are difficult to diffuse

TABLE I
Gas Phase Ethylene Polymerization Results of Different Catalysts

Catalyst	Ti (wt %)	$P_{H_2}/P_{C_2H_4}$	Catalyst activity (kg PE mol^{-1} Ti h^{-1})	M_w ($\times 10^{-5}$)	PDI	MFI [g/10 min]	Melting Point (°C)
HC-0	1.75	0.33	815	1.0	5.9	85	132.700
HC-5	1.94	0	487	4.5	8.3	/	–
HC-5	1.94	0.14	784	2.1	6.4	6.5	–
HC-5	1.94	0.33	679	1.2	8.6	76	133.100
HC-5	1.94	0.5	97	0.8	8.0	240	–
HC-20	2.07	0	933	6.8	11.5	/	–
HC-20	2.07	0.14	1092	4.2	8.9	2.8	–
HC-20	2.07	0.33	2071	2.8	8.2	9	134.033
HC-20	2.07	0.5	179	1.7	8.1	23	–

through the polyethylene to contact the inside active centers, leading to lower activities than HC-20.

In the case of ethylene polymerization, it has been generally accepted that the activity of titanium-based Ziegler-Natta catalyst decreases with the addition of hydrogen. Some different results are found in the systems currently studied. The effect of hydrogen on the polymerization was investigated by changing $P_{H_2}/P_{C_2H_4}$ from 0.0 to 0.5. Figure 5 shows that the activities of the two hybrid catalysts increase firstly and then decrease with the increase of $P_{H_2}/P_{C_2H_4}$. It is reasonable to believe that the presence of hydrogen promotes the formation of active centers on PSA layer. Therefore, the polymerization activity increases to some extent.[27,28] However, as the polymerization proceeds, hydrogen will continue to penetrate the polymer layer to reach $TiCl_3/MgCl_2$/THF of which activity normally decreases in the presence of H_2.[29] Much more hydrogen will contact $TiCl_3/MgCl_2$/THF leading to significant reduction in activity when $P_{H_2}/P_{C_2H_4}$ is higher. This explains why the overall activities of the two hybrid catalysts increase at low hydrogen content and decrease at high hydrogen content. As shown in Figure 5, HC-5 achieves the maximum activity when $P_{H_2}/P_{C_2H_4}$ is 0.14 and HC-20 achieves the maximum activity when $P_{H_2}/P_{C_2H_4}$ is 0.33. In principle, PSA layer of 5.0 μm in HC-20 increases the diffusion resistance for hydrogen. As a result, less hydrogen could reach the interior active sites in HC-20 than HC-5 and HC-20 could reach the maximum activity with more H_2 content.

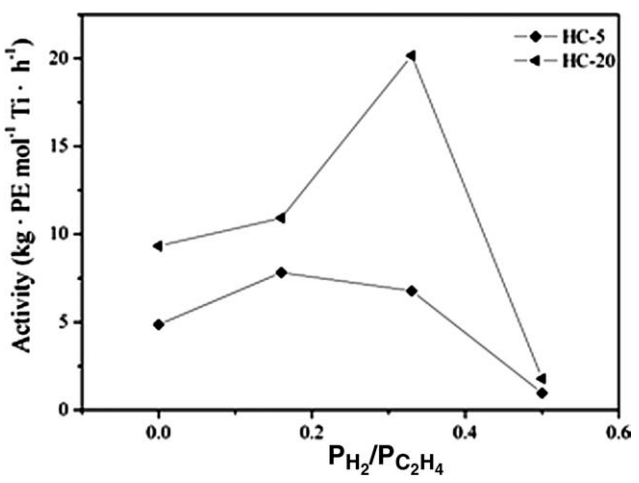

Figure 5 Effect of hydrogen on polymerization activity of different catalysts.

Physical properties of polyethylene

The core-shell hybrid catalysts produced polyethylene with higher MW compared to the catalyst without PSA, and MW showed a distinctly upward trend with the increasing thickness of the PSA layer in the same presence of hydrogen. Polymer-supported titanium-based Ziegler-Natta catalyst producing polyethylene with higher MW than $MgCl_2$-supported catalyst was concluded by Sun.[27,28] It is reasonable to believe that $TiCl_4/MgCl_2$/PSA produces polyethylene with higher MW than $TiCl_3/MgCl_2$/THF. With the growing PSA layer, more $TiCl_4/MgCl_2$/PSA exists in the hybrid catalysts, so the relative amount of high MW polyethylene in the synthesized polyethylene increases. Moreover, the diffusion resistance for the reactants increases as the PSA layer becomes thicker, leading to lower activity of the inner catalyst and the relative amount of low MW polyethylene decreases. Consequently, polyethylene produced by HC-20 obtains the highest MW. Hydrogen is widely used in Ziegler-Natta polymerizations to regulate the MW of polymer. As expected, the MW of the polymer produced by the hybrid catalysts decrease with the increase of $P_{H_2}/P_{C_2H_4}$ in Table I.

The polyethylene synthesized by the hybrid catalysts obtains broader MWD. As listed in Table I, PDI of the polyethylene produced by the catalyst without PSA is 5.9 while PDI of the polyethylene produced by the hybrid catalysts is more than 8, even achieved 11.5. More kinds of active centers forming in the hybrid catalysts and the diffusion resistance from the PSA layer are attributed to the broadened MWD

of the polyethylene produced by the hybrid catalysts. PSA with —COOH group has polarity strength different from $MgCl_2$ and exert some distinct influence on the chemical environments around the active sites. As a result, new kinds of active centers with different properties can be synthesized in the hybrid catalysts. Additionally, the diffusion resistance to different reactants from the PSA layer is not the same, leading to different TEA concentration and H_2/C_2H_4 molar ratio inside and outside the PSA layer. Therefore, polyethylene with different MW is produced and MWD becomes broad.

PDI of the polyethylene produced in the presence of H_2 are smaller than that produced in the absence of H_2, as shown in Table I. The narrower PDI is attributed to the difference in polymer chain transfer mechanism for $TiCl_3/MgCl_2/THF$ and $TiCl_4/MgCl_2/PSA$. It is likely that the chain transfer to H_2 is easier to take place in the ethylene polymerization catalyzed by $TiCl_4/MgCl_2/PSA$ than by $TiCl_3/MgCl_2/THF$. So the MW of polyethylene produced by $TiCl_4/MgCl_2/PSA$ would decrease more than that by $TiCl_3/MgCl_2/THF$. As a result, the MWD of the polyethylene synthesized by hybrid catalysts is narrower in the presence of H_2. Further investigation will be necessary to substantiate chain transfer mechanisms for the hybrid catalysts.

The polymer melt flow index (MFI) was measured as the signature for the MW of polyethylene. As expected, MFI of the polymer synthesized by hybrid catalysts are always smaller than that synthesized by the catalyst without PSA in the same presence of hydrogen. According to the above MFI results, it is deduced that the polyethylene produced by HC-5 and HC-20 obtain higher MW than that by HC-0, which agrees well with the GPC data. Polyethylene produced by HC-20 obtains the smallest MFI, indicating that it has the highest MW. The rapid increase in MFI with more hydrogen content in polymerization is probably due to the reduction of polyethylene MW.

From DSC measurements, the thermal properties of the polyethylene obtained in this study were investigated. The DSC results are listed in Table I. When $P_{H_2}/P_{C_2H_4}$ is 0.33, the melting point of the polyethylene produced by HC-0, HC-5 and HC-20 is 132.700, 133.100, and 134.033°C, respectively. It is indicated that the melting point of the resulting polyethylene improves as the PSA layer becomes thicker. As the GPC data and MFI results reported in Table I, it is certain that the catalyst with thicker PSA layer could produce polyethylene with higher MW. So, the increase of the melting point is attributed to more composition of high MW polyethylene. Undoubtedly, the polyethylene produced by HC-20 showing the highest melting point is due to the thickest PSA layer among the three catalysts.

The morphology of the resulting polyethylene

Figure 6 provides the SEM photographs of the resulting polyethylene. The morphologies of the polyethylene display the spherical shape, indicating that the replication of spherical catalyst morphology has been successfully achieved. The PSA layer does not damage the spherical shape of the catalyst and the polyethylene resin. The secondary polymer pellets of the resin synthesized by HC-0 show a homogeneous structure leading to a uniform and dense surface. The configuration of the secondary polyethylene pellets changes from homogeneity to heterogeneity [Fig. 6(a, c, and e)] by increasing the thickness of the PSA layer in the catalyst. The surface of the resin particles produced by HC-20 is loose and the shape of the secondary polymer pellets is irregular. The interstice between individual pellets is broadened with the thicker PSA layer. Obviously, the PSA layer in the hybrid catalysts influences the fragmentation behavior in the ethylene polymerization process. The unstable diffusion of the reactants and the oscillating catalytic activity in HC-20 imply that the growth of polyethylene particle is not uniform during the polymerizations.

Many fiber-like threads are observed among the polymer globules in the magnifying morphology of the powder synthesized by HC-0 [Fig. 6(b)], but none in polyethylene synthesized by HC-5 [Fig. 6(d)] and HC-20 [Fig. 6(f)]. The thermal runaway on particle scale is supposed to result in the fiber-like threads. The thermal runaway is easier to occur in the polymerization of HC-0 as the initial activity of HC-0 is high enough. The polyethylene, especially the low MW or the amorphous parts, on the particle surface is fused together and the fiber drawing occurs in the process of particle fragmentation. Generally, the initial polymerization rate of HC-5 and HC-20 is lower than that of HC-0. Moreover, polyethylene produced by $PSA/MgCl_2/TiCl_4$ has high MW. As a result, thermal runaway on particle scale hardly happens in the polymerization of the hybrid catalysts and no fiber-like threads exist on the surface of polyethylene particle.

CONCLUSIONS

Polymer-coated carrier, containing silica (SiO_2) as core and poly(styrene-*co*-acrylic acid) (PSA) as shell was successfully synthesized by the phase inversion method. Hybrid titanium catalysts ($TiCl_3/MgCl_2/THF/SiO_2{\cdot}TiCl_4/MgCl_2/PSA$) named HC-5 and HC-20 were obtained by loading titanium-based catalyst on the resulting core-shell carrier. The mass ratio of PSA/SiO_2 in HC-5 and HC-20 was 5.0% and 20.0%, respectively. The characterization results from FTIR, SEM and laser scattering particle analyzer demonstrated that the PSA content in the hybrid catalyst

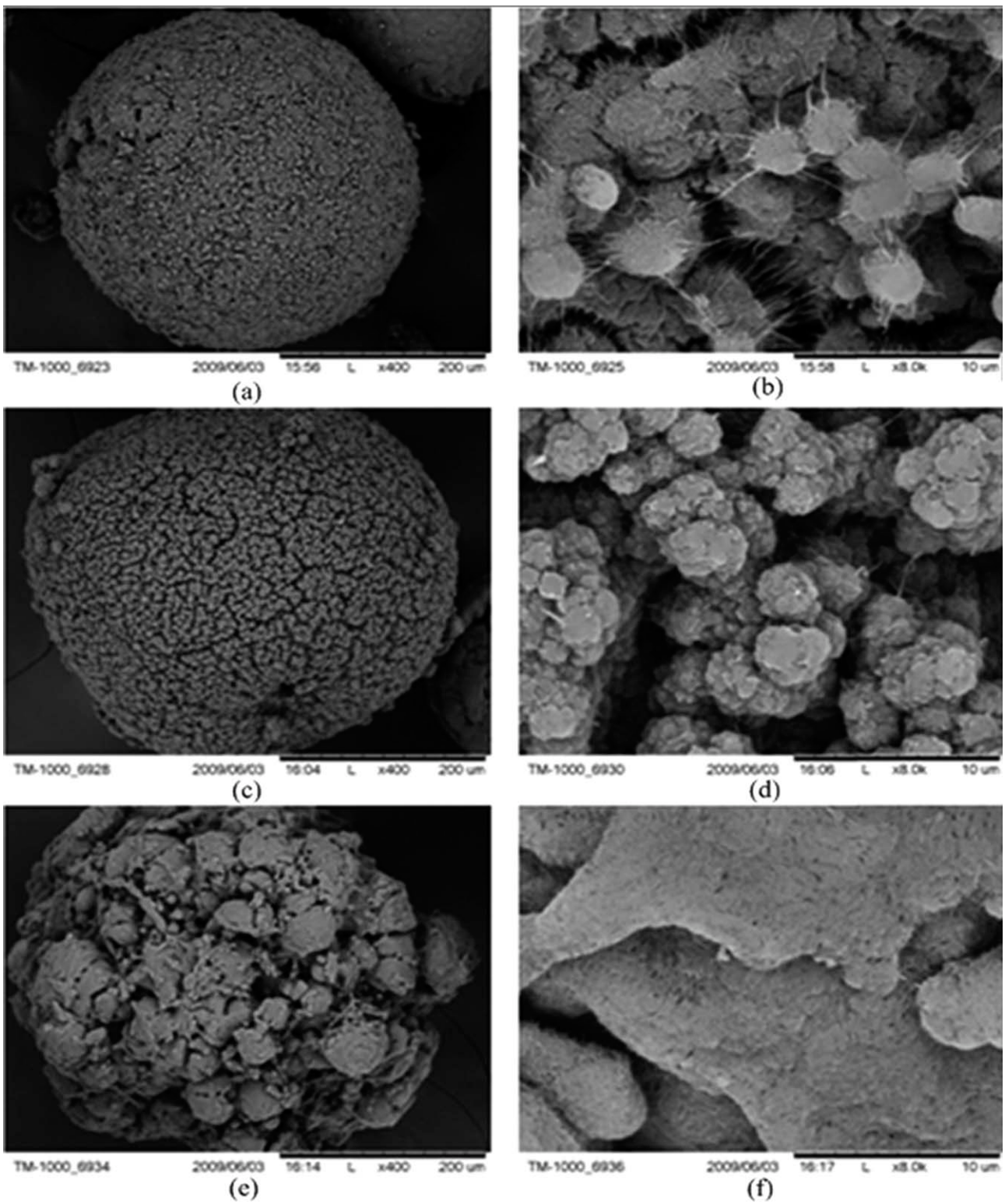

Figure 6 SEM photographs of polyethylene by HC-0 (a,b), HC-5 (c,d) and HC-20 (e,f).

influenced the surface morphology of the hybrid catalyst and the thickness of the PSA layer. The thickness of the PSA layer in HC-5 and HC-20 was 2.0 and 5.0 μm, respectively.

Ethylene homopolymerization in gas phase was carried out to investigate the influences from the PSA layer on polymerization behavior of the hybrid catalysts and the properties of the resulting polymer. Due to the PSA layer serving as the diffusion barrier for the reactants, the thickness of PSA layer strongly affected the trend of the kinetic curves. HC-0 with no PSA layer and HC-5 with the PSA layer of 2.0 μm

showed typically decay-type kinetics while HC-20 with the PSA layer of 5.0 μm obtained kinetic curve with a diffusion-controlled inductive period. Furthermore, the kinetic curve of HC-20 was steadier and obtained longer polymerization life time than the other two catalysts. The activities of the hybrid catalysts were comparable to the conventional titanium-based Ziegler-Natta catalyst ($TiCl_3/MgCl_2/THF/SiO_2$), enhancing firstly and then decreasing with the increase of $P_{H_2}/P_{C_2H_4}$. The polyethylene produced by the hybrid catalysts obtained higher MW and broader MWD. Both the MW and MWD of the resulting polyethylene reflected a distinctly upward trend with the increasing thickness of the PSA layer. As the thickness of the PSA layer was the key effect, it was reasonable to conclude that HC-20 with the thickest PSA layer obtained the longest polymerization life time with the highest activity (2071 kg PE mol^{-1} Ti h^{-1}) and the resulting polyethylene had the broadest MWD (polydispersity index = 11.5) under our experimental conditions.

We can further broaden the MWD of polyethylene by varying the matching mass ratio of the catalysts and polymerization condition. The copolymerization of ethylene and 1-hexene will be carried out in our laboratory to investigate the "filtration effect" to 1-hexene and how the membrane will influence the properties of the ethylene-*co*-1-hexene copolymer. We are also planning to design the hybrid catalyst, combining Ziegler-Natta[27,28] catalyst and metallocene catalyst on this core-shell carrier, to obtain bimodal polyethylene.

References

1. Ray, W. H.; Soares, J. B. P.; Hutchinson, R. A. Macromol Symp 2004, 206, 1.
2. De Souza, R. F.; Casagrande, O. L. Macromol Rapid Commun 2001, 22, 1293.
3. Wang, J. F.; Wang, L.; Gao, H. Q.; Wang, W. Q.; Zhao, Z. R.; Sun, T. X.; Feng, L. F. Polym Int 2006, 55, 299.
4. Liu, H. T.; Davey, C. R.; Shirodkar, P. P. Macromol Symp 2003, 195, 309.
5. Kim, J. D.; Soares, J. B. P.; Rempel, G. L. J Polym Sci Part A: Polym Chem 1999, 37, 331.
6. Ahmadi, M.; Jamjah, R.; Nekoomanesh, M.; Nekoomanesh, M.; Zohuri, G. H.; Arabi, H. Macromol React Eng 2007, 1, 604.
7. Camargo Forte, M. M.; Cunha, F. V.; Santos, J. H. Z. J Mol Catal A: Chem 2001, 175, 91.
8. Camargo Forte, M. M.; Cunha, F. V.; Santos, J. H. Z.; Zacca, J. J Polym 2003, 44, 1373.
9. Chung, J. S.; Cho, H. S.; Ko, Y. G.; Lee, W. Y. J Mol Catal A: Chem 1999, 144, 61.
10. Cho, H. S.; Chung, J. S.; Lee, W. Y. J Mol Catal A: Chem 2000, 159, 203.
11. Cho, H. S.; Choi, Y. H.; Lee, W. Y. Catal Today 2000, 63, 523.
12. Sung, C. H.; Mihan, S.; Lilge, D.; Detux, L.; Rief, U. Polym Eng Sci 2007, 47, 131.
13. Caruso, F. Adv Mater 2001, 13, 11.
14. Fleming, M. S.; Mandal, T. K.; Walt, D. R. Chem Mater 2001, 13, 2210.
15. Sertchook, H.; Avnir, D. Chem Mater 2003, 15, 1690.
16. Wang, Y. J.; Xiong, Y.; Chen, F.; Luo, G. S. J Appl Polym Sci 2006, 99, 3365.
17. Zhang, K.; Chen, H. T.; Chen, X.; Chen, Z. H.; Cui, Z. C.; Yang, B. Macromol Mater Eng 2003, 288, 380.
18. Luo, H. L.; Sheng, J.; Wan, Y. Z. Mater Lett 2008, 62, 37.
19. Chen, C. W.; Chen, M. Q. Chem Commun 1998, 7, 831.
20. Chen, C. W.; Serizawa, T.; Akashi, M. Chem Mater 1999, 11, 1381.
21. Liu, C. B.; Tang, T.; Huang, B. T. J Polym Sci Part A: Polym Chem 2001, 39, 2085.
22. Guo, Y.; Zhang, X. Q.; Dong, W. M. J Mol Catal A: Chem 2005, 237, 45.
23. Zhang, D.; Jin, G. X. Appl Catal A 2004, 262, 18.
24. Mulder, M. Basic Principles of Membrane Technology; 2nd ed.; Kluwer Academic Publishers: The Netherlands, 1996, p 89.
25. Machado, P. S. T.; Habert, A. C.; Borges, C. P. J Membr Sci 1999, 155, 171.
26. Przybyla, C.; Tesche, B.; Fink, G. Macromol Rapid Commun 1999, 20, 328.
27. Sun, L.; Hsu, C. C.; Bacon, D. W. J Polym Sci Part A: Polym Chem 1994, 32, 2135.
28. Sun, L.; Hsu, C. C.; Bacon, D. W. J Polym Sci Part A: Polym Chem 1994, 32, 2127.
29. Czaja, K.; Bialeck, M. J Appl Polym Sci 2001, 79, 961.